Donor and acceptor levels in semiconducting transition-metal dichalcogenides

A. Carvalho and A. H. Castro Neto

Graphene Research Center, National University of Singapore, 6 Science Drive 2, Singapore 117546[*]
(Received 5 November 2013; revised manuscript received 7 January 2014; published 25 February 2014)

Density functional theory calculations are used to show that it is possible to dope semiconducting transition-metal dichalcogenides (TMD) such as MoS_2 and WS_2 with electrons and/or holes either by chemical substitution or by adsorption on the sulfur layer. Notably, the activation energies of lithium and phosphorus, a shallow donor and a shallow acceptor, respectively, are smaller than 0.1 eV. Substitutional halogens are also proposed as alternative donors adequate for different temperature regimes. All dopants proposed result in very little lattice relaxation and, hence, are expected to lead to minor scattering of the charge carriers. Doped MoS_2 and WS_2 monolayers are extrinsic in a much wider temperature range than 3D semiconductors, making them superior for high temperature electronic and optoelectronic applications.

Advances in the fabrication and characterization of two-dimensional (2D) dichalcogenide semiconductors have reshaped the concept of thin transistor gate [1,2]. Unlike thin fully-depleted silicon channels, physically limited by the oxide interface, single layer metal dichalcogenides are intrinsically 2D and, therefore, have no surface dangling bonds. The monolayer thickness is constant, and the scale of the variations of the electrostatic potential profile perpendicular to the plane is only limited by the extent of the electronic wave functions. Hence, TMD can in principle be considered immune to channel thickness modulation close to the drain.

Building on these fundamental advantages, numerous field-effect transistor (FET) designs employing MoS_2 or WS_2 channels have been proposed. These range from 2D adaptations of the traditional FET structure, where the 2D semiconductor is separated by a dielectric layer from a top gate electrode, to dual-gate heterolayer devices where the transition-metal dichalcogenide is straddled between two graphene sheets [2]. Such FETs can be integrated into logic inversion circuits, providing the building blocks for all logical operations [3].

However, at present the success of TMD in electronics is limited by the difficulty in achieving high carrier concentrations and, by consequence, high electronic mobilities (most recent values range around 100 cm^2/V.s) [4]. In the absence of a chemical doping technology, the control of the carrier concentration relies solely on the application of a gate voltage perpendicular to the layer, which shifts the Fermi level position rendering the material n- or p-type [5]. But in practice the gate voltage drop across the insulator cannot exceed its electric breakdown limit (about 1 V/nm for SiO_2, or lower for high-κ dielectrics [6]). A work around demonstrated in graphene consists of gating with ferroelectric polymers [7], although at the expense of the thermal stability and switching time.

In this Rapid Communication we use first-principles calculations to show that MoS_2 and WS_2 can be doped both n- and p-type using substitutional impurities. This grants transitional metal dichalcogenides an advantage over other chalcogenide semiconductor families where doping asymmetries are notorious: ZnS can be doped n-type but

not p-type, while chalcopyrite $CuInTe_2$ and $CuGaSe_2$ can be p-type doped but not n-type doped [8], and SnTe has not yet been doped n-type [9]. In transition-metal dichalcogenides, even though chemical doping is mostly unexplored, there have already been some experimental reports of successful chemical doping [10,11], as well as some electronic structure calculations for impurities [12–15].

Further, we propose both n- and p-type dopants substituting *in the S lattice site* or adsorbed *on top* of the S layer. Leaving the transition-metal layer nearly undisturbed, these substitutions promise less scattering to charge carriers at the Mo-derived states at the bottom of the conduction band (CBM) or at the top of the valence band (VBM).

Having established that doping is possible, it follows that 2D doped semiconductors stand out as superior to 3D semiconductors for high temperature applications because of the fact that the electronic density of states $N(E)$ close to the edge of the valence and conduction bands is, unlike the 3D case, energy independent. It is well known that the intrinsic carrier concentration of a semiconductor is given by:

$$n_i(T) = \sqrt{N_c(T)N_v(T)}\exp\left(-E_g/(2kT)\right), \quad (1)$$

where E_g is the gap energy, and $N_{c(v)}$ depend on $N(E)$ (and hence the dimensionality) of the semiconductor. In 2D we have:

$$N_{c(v)} = \frac{M_{c(v)}m_{e(h)}\ln 2}{\pi\hbar^2}kT, \quad (2)$$

where $M_{c(v)}$ is the degeneracy of the conduction (valence) band, $m_{e(h)}$ is the effective mass for electrons (holes), and T is the temperature (k and $\hbar$ are the Boltzmann and Planck's constants, respectively). Hence, in 2D we have $n_{i,2D}(T) \propto T$ which should be contrasted against the 3D counterpart where $n_{i,3D} \propto T^{3/2}$. Figure 1 illustrates the relevance of the temperature dependence of the density of conduction electrons $n(T)$ by comparing the carrier density for n-type monolayer MoS_2 and Si, doped with the same dopant concentration and dopant activation energy, as a function of temperature. While Si leaves the extrinsic regime [that is, the region of temperatures where $n_i(T)$ becomes temperature independent] above 800 K, in MoS_2 the $n(T)$ curve is flat beyond 1000 K. The temperature stability of n_i ultimately reflects on transistor characteristics, in particular the gate voltage threshold.
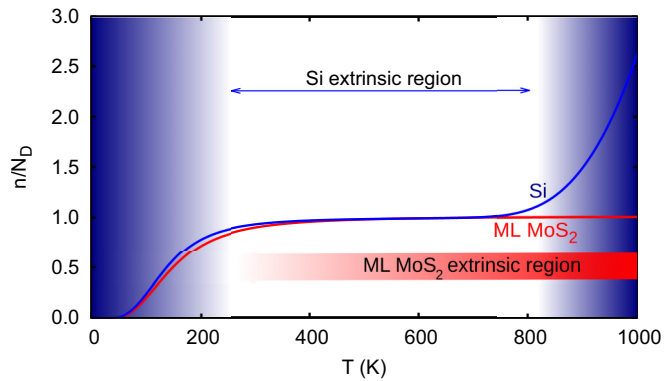
---

[*]physdca@nus.sg.edu

FIG. 1. (Color online) Electron density in n-type monolayer MoS$_2$ and Si, with concentration $N_D = 10^{18}$ cm^{-3} of donors with ionization energy $E_c - E_I = 0.045$ eV. An effective thickness of 6.46 Å was used for MoS$_2$.

We studied donor and acceptor impurities using first-principles calculations. These were based on density functional theory (DFT), as implemented in the QUANTUM ESPRESSO code [16]. Geometry optimizations and total energy calculations are nonrelativistic. A fully relativistic formalism was used for the band-structure calculations [17]. The exchange correlation energy was described by the generalized gradient approximation (GGA), in the scheme proposed by Perdew-Burke-Ernzerhof [18] (PBE). The Kohn-Sham band gaps obtained in the nonrelativistic calculations are, respectively, 1.65 and 1.77 eV for MoS$_2$ and WS$_2$. With spin orbit coupling, these values become 1.55 and 1.51 eV, respectively. We thus find that the GGA is a good approach for band-structure calculations of these materials, and further exchange and correlation effects are likely to produce, in first approximation, only a rigid shift of the conduction band [19]. The energy cutoff used was 50 Ry. Further details of the calculation method can be found in Ref. [20].

The supercell consisted of 4×4 unit cells of the single layer material, separated by a vacuum spacing with the thickness of two times the supercell lattice parameter. For charged supercells, the electrostatic correction of Komsa and Pasquarello was implemented [21,22]. The Brillouin zone (BZ) was sampled using a $4 \times 4 \times 1$ Monkhorst-Pack grid [23].

We have considered five dopants: Si, P, Li, Br, and Cl. Any of these can either occupy substitutional positions or be adsorbed on the S layer. The point symmetry of the S site is C_{3v}. When replaced by P or Si, the resulting defect keeps the trigonal symmetry and there is little associated lattice distortion. In the case of neutral Cl$_S$ and Br$_S$ however, the lowest energy configuration is a C_s geometry where the neutral Cl$_S$ and Br$_S$ defects are displaced in the vertical plane, loosening one of the Cl/Br-Mo/W bonds [Fig. 2(a)]. This unusual configuration results from the fact that the halogen partially donates the unpaired electron to the Mo/W d orbitals, whereas in most molecules Cl and Br receive an electron instead.

Li is most stable at the S3 position [13], shown in Fig. 2(b), outside the S layer but on the top of a Mo atom. As for the
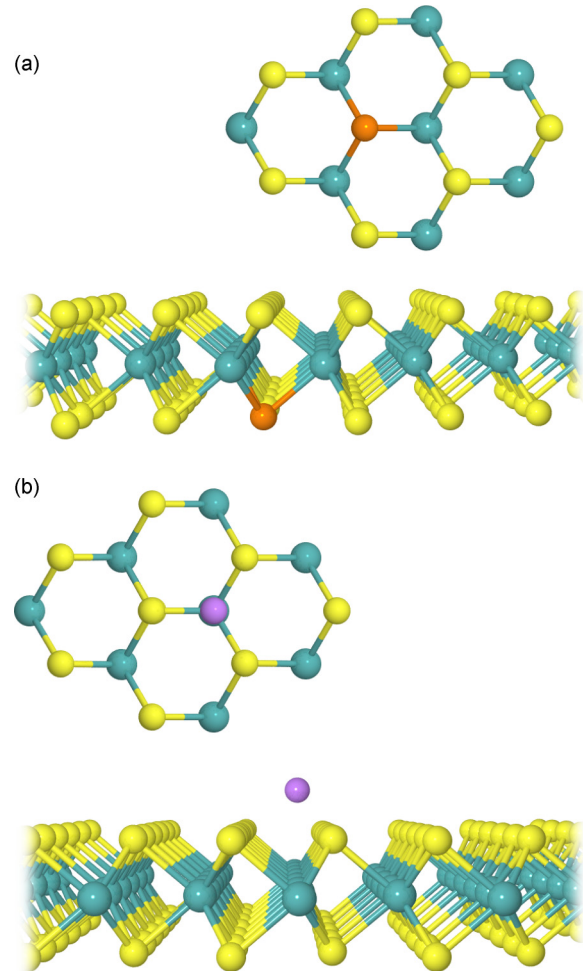

FIG. 2. (Color online) Top: geometry of a distorted substitutional defect (Br$_S$), in top and side view. Bottom: geometry of Li adsorbed at the S3 position. TM and S atoms are represented as gray and white spheres, respectively.

adsorbed atoms, P, Si, Cl, and Br take the S4 configuration as described in Ref. [13], on top of an S atom.

A requirement for successful doping is that the impurity must be stable at the lattice position where it is active, and comparatively unstable or electrically neutral at the competing positions. The equilibrium concentration $[D]$ of a defect form D can be related to the defect formation energy ΔG_D,

$$[D] = gN_D \exp\left(-\frac{\Delta G_D}{kT}\right), \qquad (3)$$

where N_D is the number of sites available to the defect.

Since our calculations are for $T = 0$ entropy terms can be neglected, and the formation energy of the defect can be obtained from the total energies,

$$\Delta G_D \simeq E_f(D) = E(D) - \sum_i n_i \mu_i + q\mu_e, \qquad (4)$$

where $E_f(D)$ is the free energy of the system containing the defect, n_i is the number of atoms of species i that it contains, and μ_i is the respective chemical potential. Additionally, the formation energy of a charged system, in charge state q, depends on the chemical potential of the electrons (μ_e).

TABLE I. Formation energy of substitutional impurities (E_f) along with adsorption energies. All values are in eV and refer to the neutral charge state.

Defect	MoS$_2$		WS$_2$	
	$E_f^{\text{S-poor}}(D_S)$	$E_f(D_{\text{ad}})$	$E_f^{\text{S-poor}}(D_S)$	$E_f(D_{\text{ad}})$
Br$_S$	-1.0	-0.7	-0.3	-0.7
Cl$_S$	-1.5	-0.9	-0.9	-0.9
Li$_S$	-0.7	-2.0	-0.9	-1.5
P$_S$	-2.9	-0.7	-2.7	-0.6
Si$_S$	-2.6	-1.6	-2.0	-0.9

The chemical potentials are defined by the experimental growth conditions, which can range from metal-rich to sulfur-rich. Bulk MoS$_2$ and WS$_2$ are often sulfur deficient [24,25], even though sulfur excess has been reported as well [26]. Here, we will assume $\{\mu_{\text{Mo/W}}, \mu_S\}$ are in the metal-rich extreme, i.e., the system is in equilibrium with a hypothetical reservoir of metallic Mo (or W). The chemical potentials for the impurities are taken to be the total energy of the respective isolated atoms, so that $E_f(D_{\text{ad}})$ is by definition the adsorption energy.

The calculated formation energies are given in Table I. We note that for the defects in MoS$_2$ there is a good agreement with the values obtained in Ref. [14] using hybrid functionals. In the sulfur-poor limit, for both host materials, substitutional Si and P bind strongly to the lattice, and are more stable in the substitutional position. Li, on the contrary, is most stable at a surface adsorbed position. (See Fig. 3.)

Br and Cl have comparable formation energies in both forms. The energy difference between adsorption and substitution at the S site is linear on the chemical potential of sulfur, and independent on the chemical potential of the impurity itself:

$$E_f(D_S) - E_f(D_{\text{ad}}) = E(D_S) - E(D_{\text{ad}}) + \mu_S. \quad (5)$$

Thus, it is in principle possible to control the relative populations of Cl or Br in different sites by changing the sulfur abundance.

Another way to enhance the incorporation ratio of Br and Cl at S sites is by using material that has sulfur vacancies
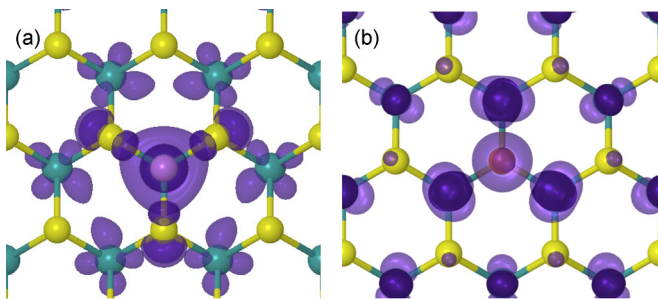

FIG. 3. (Color online) Isosurfaces of the unpaired electron state of Li$_{\text{ad}}$ (a) and of the unpaired hole state of P$_S$ (b), in MoS$_2$, as generated by fully relativistic calculations. The former is a donor, whereas the latter is an acceptor. The square of the wave function is represented. W and S are represented by cyan and yellow spheres, respectively.

a priori (for example pre-irradiated material). The capture of an impurity atom X adsorbed at the layer surface by a sulfur vacancy,

$$V_S + X_{\text{ad}} \rightarrow X_S, \quad (6)$$

where V_S is the sulfur vacancy and X_{ad} is the adsorbed atom is isoenthalpic for Br and Cl. Furthermore, for Cl the respective energy gain is actually greater than the formation energy of the vacancy (1.3 and 1.7 eV in sulfur-poor MoS$_2$ and WS$_2$, respectively).

We have so far considered the stability of the neutral defects. Now the most important requirement for a dopant is that its ionization energy E_I^D is not greater than a few kT. The thermodynamic transition level $E_D(q/q+1)$ can be defined as the value of the Fermi level for which charge states q and $q+1$ of the defect D have the same formation energy. The position of the $E_D(q/q+1)$ level relative to the valence band top E_v can be found from the formation energies [see Eq. (4)] [27]

$$E_D(q/q+1) = E_f[X^q] - E_f[X^{q+1}] - E_v. \quad (7)$$

Thus for acceptors $E_D(0/+) \equiv E_I^D$ and for donors $E_D(-/0) \equiv E_g - E_I^D$.

For comparison, we have also calculated the same defect levels using the marker method (MM). In this method, the ionization energies/electron affinities of defective supercells are compared with those of the pristine supercell [28], and the spurious electrostatic interactions are partially canceled. There is good agreement between the levels calculated using the two methods, in most cases within about 0.1 eV. Another indication of the quality of the method is the agreement between the gap obtained from total energy difference $\tilde{E}_g = E_S(+) + E_S(-) - 2E_S(0) - 2\delta_E$, where $E_S(q)$ is the energy of the pristine supercell in charge state q and δ_E is the electrostatic correction of Ref. [21], and the Kohn-Sham gap. These are, respectively, $\tilde{E}_g = 1.64$ and 1.87 eV for MoS$_2$ and WS$_2$, and $E_g = 1.65$ and 1.77 eV for MoS$_2$ and WS$_2$.

Adsorbed Li is a shallow donor with a small ionization energy <0.1 eV both in MoS$_2$ and WS$_2$. This is mainly due to two effects. First, the relaxation of Li in the positive charge state, which is of the order of 30 meV and is a physical effect; second, a spurious band filling effect [29,30], which is estimated to be largest for Li$_{\text{ad}}$ in WS$_2$ (~ 0.2 eV) due to the greatest dispersion of the lowest conduction band. The band structure shows unequivocally that Li$_{\text{ad}}$ is a shallow donor [17]. In effect, it merely gives out an electron to the conduction band, changing little the matrix band structure in the vicinity of the gap (see Fig. 1 of Supplemental material [17]).

Substitutional Br and Cl are shallow donors only above room temperature. They contribute with an additional electron to populate a perturbed conduction band state. The shallowest of them is Br$_S$, with an ionization energy of about 0.1–0.2 eV both in MoS$_2$ and WS$_2$ (Table II). Even though this is higher than the ionization energy of shallow dopants in bulk materials such as Si or GaAs, it is lower than the dopant ionization energies in layered BN [31].

Substitutional P is found to be a very shallow acceptor, with activation energy ~ 0.1 eV in MoS$_2$, and <0.1 eV in WS$_2$, comparable to the uncertainty of the calculation. Si is also an acceptor, though deeper. It is noticeable that ionization energies in WS$_2$ are usually smaller, despite its

TABLE II. Defect-related levels in MoS_2 and WS_2. $E(-/0)$ is given relative to E_v and $E(0/+)$ is given relative to E_c. FEM and MM stand for formation energy method and marker method, respectively (see text). All values are in eV.

	MoS_2			
	$(-/0)$	$(-/0)$	$(0/+)$	$(0/+)$
Method	FEM	MM	FEM	MM
Br_S			0.15	0.22
Cl_S			0.18	0.27
Li_{ad}			-0.02	0.12
P_S	0.11	0.06		
Si_S	0.39	0.34		
	WS_2			
	$(-/0)$	$(-/0)$	$(0/+)$	$(0/+)$
Method	FEM	MM	FEM	MM
Br_S			0.14	0.14
Cl_S			0.18	0.22
Li_{ad}			-0.36	-0.16
P_S	0.02	-0.09		
Si_S	0.23	0.12		

larger calculated band gap, suggesting that this material is easier to dope.

In summary, we have shown that it is possible to dope MoS_2 and WS_2 with electrons or holes by chemical substitution at the S site or adsorption on the top of the layer. Amongst the shallow donors, Li_{ad} has the lowest ionization energy. The donated electron is predominantly localized on the transition-metal d states. However, Li diffuses extremely fast in most materials and therefore is not a good choice for high temperature applications. Besides, Br_S and Cl_S are also donors, but have a higher ionization energy. The higher temperature required to excite the carriers is a tradeoff for the higher temperature stability of the defects.

Phosphorus is a shallow acceptor with a very low ionization energy, comparable to the uncertainty of the calculation. The wave function of the unpaired hole state is a valence-band-like state, predominantly localized on the transition-metal layer. This suggests that the ionized P_S defect will be a weak scattering center. The combination of the high stability of P and the fact that it contributes with a very delocalized electron to the material, preserving the characteristics of a 2D electron gas, indicates that its extrinsic region would extend up to much higher temperatures than for Si, that readily becomes intrinsic at about 800 K (Fig. 1).

These findings open the way to the control of the conductivity type in these two materials, offering a way to use MoS_2 and WS_2 for transistor parts other than the channel, or even to integrate different functionalities in the same layer. This seems extremely promising for the design of electronic and optoelectronic devices for high temperature operation.

[1] M. Chhowalla, H. S. Shin, G. Eda, L.-J. Li, K. P. Loh, and H. Zhang, Nat. Chem. **5**, 263 (2013).

[2] Q. H. Wang, K. Kalantar-Zadeh, A. Kis, J. N. Coleman, and M. S. Strano, Nat. Nanotechnol. **7**, 699 (2012), and references therein.

[3] B. Radisavljevic, M. B. Whitwick, and A. Kis, ACS Nano. **5**, 9934 (2011).

[4] B. Radisavljevic, A. Radenovic, J. Brivio, V. Giacometti, and A. Kis, Nat. Nanotechnol. **6**, 147 (2011).

[5] W. Bao, X. Cai, D. Kim, K. Sridhara, and M. S. Fuhrer, Appl. Phys. Lett. **102**, 042104 (2013).

[6] C. Sire, S. Blonkowski, M. J. Gordon, and T. Baron, Appl. Phys. Lett. **91**, 242905 (2007).

[7] G.-X. Ni, Y. Zheng, S. Bae, C. Y. Tan, O. Kahya, J. Wu, B. H. Hong, K. Yao, and B. Özyilmaz, ACS Nano **6**, 3935 (2012).

[8] Y.-J. Zhao, C. Persson, S. Lany, and A. Zunger, Appl. Phys. Lett. **85**, 5860 (2004).

[9] D. J. Singh, Functional Materials Letters **1**, 1 (2008).

[10] H. Fang, M. Tosun, G. Seol, T. C. Chang, K. Takei, J. Guo, and A. Javey, Nano Lett. **13**, 1991 (2013).

[11] Y. Du, H. Liu, A. T. Neal, M. Si, and P. D. Ye, IEEE Electron Device Letters **34**, 1328 (2013).

[12] H.-P. Komsa, J. Kotakoski, S. Kurasch, O. Lehtinen, U. Kaiser, and A. V. Krasheninnikov, Phys. Rev. Lett. **109**, 035503 (2012).

[13] C. Ataca and S. Ciraci, J. Phys. Chem. C **115**, 13303 (2011).

[14] K. Dolui, I. Rungger, C. Das Pemmaraju, and S. Sanvito, Phys. Rev. B **88**, 075420 (2013).

[15] H.-P. Komsa, S. Kurasch, O. Lehtinen, U. Kaiser, and A. V. Krasheninnikov, Phys. Rev. B **88**, 035301 (2013).

[16] P. Giannozzi, S. Baroni, N. Bonini, M. Calandra, R. Car, C. Cavazzoni, D. Ceresoli, G. L. Chiarotti, M. Cococcioni, I. Dabo, A. Dal Corso, S. Fabris, G. Fratesi, S. de Gironcoli, R. Gebauer, U. Gerstmann, C. Gougoussis, A. Kokalj, M. Lazzeri, L. Martin-Samos, N. Marzari, F. Mauri, R. Mazzarello, S. Paolini, A. Pasquarello, L. Paulatto, C. Sbraccia, S. Scandolo, G. Sclauzero, A. P. Seitsonen, A. Smogunov, P. Umari, and R. M. Wentzcovitch, J. Phys.: Condens. Matter **21**, 395502 (2009).

[17] See Supplemental Material at http://link.aps.org/supplemental/10.1103/PhysRevB.89.081406 for relativistic band structures of dopants in WS_2.

[18] J. P. Perdew, K. Burke, and M. Ernzerhof, Phys. Rev. Lett. **77**, 3865 (1996).

[19] H.-P. Komsa and A. V. Krasheninnikov, Phys. Rev. B **86**, 241201(R) (2012).

[20] A. Carvalho, R. M. Ribeiro, and A. H. Castro Neto, Phys. Rev. B **88**, 115205 (2013).

[21] H.-P. Komsa and A. Pasquarello, Phys. Rev. Lett. **110**, 095505 (2013).

[22] The values of the correction for a defect in the middle of the slab, at the interface, and on the surface were 0.19, 0.21, and 0.19 eV, respectively, for MoS_2 and 0.19, 0.21, and 0.16 eV, respectively, for WS_2.

[23] H. J. Monkhorst and J. D. Pack, Phys. Rev. B **13**, 5188 (1976).

[24] T. Ito and K. Nakajima, Philosophical Magazine Part B **37**, 773 (1978).

[25] V. Wei, S. Seeger, K. Ellmer, and R. Mientus, J. Appl. Phys. **101**, 103502 (2007).

[26] M. Potoczek, Przybylski, and M. Rekas, J. Phys. Chem. Solids **67**, 2528 (2006).

[27] The value of E_v obtained from the band structure of the pristine supercell is usually corrected by alignment of the average electrostatic potentials [32]. However, since in this case a great fraction of the supercell was occupied by vacuum the alignment term was found to be negligible.

[28] J. Coutinho, V. J. B. Torres, R. Jones, and P. R. Briddon, Phys. Rev. B **67**, 035205 (2003).

[29] A. Carvalho, A. Alkauskas, A. Pasquarello, A. K. Tagantsev, and N. Setter, Phys. Rev. B **80**, 195205 (2009).

[30] S. Lany and A. Zunger, Phys. Rev. B **80**, 085202 (2009).

[31] F. Oba, A. Togo, I. Tanaka, K. Watanabe, and T. Taniguchi, Phys. Rev. B **81**, 075125 (2010).

[32] C. G. van de Walle and J. Neugebauer, J. Appl. Phys. **95**, 3851 (2004).